

This article was downloaded by:

On: 24 January 2011

Access details: *Access Details: Free Access*

Publisher *Taylor & Francis*

Informa Ltd Registered in England and Wales Registered Number: 1072954 Registered office: Mortimer House, 37-41 Mortimer Street, London W1T 3JH, UK



Journal of Macromolecular Science, Part A

Publication details, including instructions for authors and subscription information:

<http://www.informaworld.com/smpp/title~content=t713597274>

Forces between Polymer Surfaces and Self-Assembled Monolayers

Jagdeep Singh^a; James E. Whitten^a

^a Department of Chemistry and Center for High-Rate Nanomanufacturing, The University of Massachusetts Lowell, Lowell, MA

To cite this Article Singh, Jagdeep and Whitten, James E.(2008) 'Forces between Polymer Surfaces and Self-Assembled Monolayers', Journal of Macromolecular Science, Part A, 45: 11, 884 – 891

To link to this Article: DOI: 10.1080/10601320802378186

URL: <http://dx.doi.org/10.1080/10601320802378186>

PLEASE SCROLL DOWN FOR ARTICLE

Full terms and conditions of use: <http://www.informaworld.com/terms-and-conditions-of-access.pdf>

This article may be used for research, teaching and private study purposes. Any substantial or systematic reproduction, re-distribution, re-selling, loan or sub-licensing, systematic supply or distribution in any form to anyone is expressly forbidden.

The publisher does not give any warranty express or implied or make any representation that the contents will be complete or accurate or up to date. The accuracy of any instructions, formulae and drug doses should be independently verified with primary sources. The publisher shall not be liable for any loss, actions, claims, proceedings, demand or costs or damages whatsoever or howsoever caused arising directly or indirectly in connection with or arising out of the use of this material.

Forces between Polymer Surfaces and Self-Assembled Monolayers

JAGDEEP SINGH and JAMES E. WHITTEN

Department of Chemistry and Center for High-Rate Nanomanufacturing, The University of Massachusetts Lowell, Lowell, MA 01854

Gold-coated atomic force microscope (AFM) tips functionalized with amine-, hydroxyl-, carboxylic acid-, and methyl-terminated alkanethiol molecules were used to probe the adhesive forces of polystyrene and poly(acrylic acid) films in dry air (relative humidity <0.5%). X-ray photoelectron spectroscopy (XPS) and contact angle measurements confirmed the quality and uniformity of similarly treated gold surfaces and the polymer films. XPS indicated that the amine-functionalized thiol films were protonated and comprised of multilayers. Contact angle data were used to calculate surface free energies, and DMT theory yielded the works of adhesion and interfacial free energies for the tip-substrate combinations. In the case of polystyrene, the work of adhesion followed the order methyl > carboxylic acid > hydroxyl > amine. For poly(acrylic acid), the observed order was hydroxyl > amine > carboxylic acid > methyl.

Keywords: Force spectroscopy, poly(acrylic acid), polystyrene, self-assembled monolayers, surface free energy, photoelectron spectroscopy

1. Introduction

Forces of attraction and adhesion between coated surfaces are critical to a number of technological processes including papermaking, ink jet printing, particle removal, cell adhesion, and molecular assembly (1–3). Forces between functionalized surfaces are also critical for nanotechnology and nanomanufacturing applications. Recent research has demonstrated that molecular layers may be used as templates to direct the adsorption of subsequently deposited materials, including polymers, biomaterials and conjugated oligomers (4–6). Briefly, the method consists of using either microcontact printing or dip-pen nanolithography (DPN) to form hydrophilic patterns on a surface. The remainder of the surface is “backfilled” with a hydrophobic molecule. Subsequent coating and annealing of a mainly hydrophilic material results in its preferential, and often exclusive, adsorption onto the hydrophilic regions of the surface. The method is especially useful for materials that cannot be directly patterned by microcontact printing or DPN. Forces of attraction and adhesion present between the material to be coated and the template drive the process.

Toward the goals of understanding and optimizing adhesive interactions between functionalized and coated surfaces, “force-distance curves” may be measured by monitoring the deflection of the cantilever of an atomic force microscope (AFM) as a function of distance between the tip and surface (7). As the tip is brought into close proximity (<100 nm) to the surface, it may undergo attractive or repulsive forces that cause the cantilever to be deflected. If the tip and surface are brought close enough together, molecular forces between them (e.g., van der Waals, dipole-dipole, hydrogen bonding) usually lead to a small but measurable attraction. The initial attractive regime upon approach is referred to as the “jump-in” regime and results in a minimum in the force-distance curve. Upon retraction, a larger minimum is generally observed which is referred to as the “pull-off” (or adhesion) regime.

The use of self-assembled monolayers (SAMs) provides a convenient method of functionalizing surfaces in a reproducible fashion, and their applications in force studies have been previously discussed (8). In the present work, AFM has been used to measure the forces of adhesion between tips functionalized with alkanethiol monolayers and spin-coated polystyrene and poly(acrylic acid) surfaces. Surfaces functionalized with 11-aminoundecanethiol (AUT), 11-mercaptopundecanoic acid (MUA), 11-hydroxyundecanethiol (HUT), and octadecanethiol (ODT) have been chosen because the first three

Address correspondence to: James E. Whitten, Department of Chemistry, University of Massachusetts Lowell, One University Avenue, Lowell, MA 01854. Ph: (978) 934-3666; Fax: (978) 934-3013; E-mail: James.Whitten@uml.edu

yield hydrophilic surfaces of different character, and ODT gives a hydrophobic surface. The functionalized surfaces have been characterized with contact angle measurements and X-ray photoelectron spectroscopy (XPS), and the work of adhesion has been calculated for each tip/surface combination using DMT theory.

2. Experimental

2.1. Materials and methods

Polystyrene (MW 18,100 g/mol), poly(acrylic acid) (MW 2,000 g/mol) and octadecanethiol were purchased from Aldrich Chemical Company and used as received. 11-aminoundecanethiol hydrochloride, 11-mercaptoundecanoic acid and 11-hydroxyundecanethiol were purchased from Asemblon, Inc. and used without further purification. All other chemicals were reagent grade and used as received. Chemical structures of the relevant molecules are shown in Figure 1. Polystyrene and poly(acrylic acid) films, hereafter referred to as PS and PAA, respectively, were coated on clean Si(111) wafers (ultrasonicated in methanol and acetone prior to use) by spin-casting from 1 wt% polymer solutions (PAA in methanol and PS in toluene) at 3000 rpm for 30 sec. The prepared films were annealed in a vacuum oven at 120°C for 24 h to ensure low surface roughness of the films and evaporation of the solvent.

For XPS and contact angle measurements, gold-coated substrates were prepared by vapor depositing 30 Å of Ti and then 1500 Å of gold in a vacuum of ca. 10^{-7} Torr onto clean Si(111) wafers. Gold-coated AFM tips (CSC17/Cr-Au) were purchased from Mikromasch, Inc. The tips and gold-coated substrates were cleaned by UV-ozone treatment for 20 min. They were then immersed in 65°C ethanol for 20 min. This procedure has been shown to result in clean gold surfaces (9). Self-assembly of thiols was achieved by immersing the freshly cleaned surfaces into 1–2 mM ethanolic thiol solutions for ca. 24 h. After removal, the tips and substrates were rinsed with pure ethanol several times and dried in a stream of N₂ gas.

AFM imaging was performed in tapping mode using a Veeco Nanoscope IIIa instrument. XPS was performed in a VG ESCALAB MKII instrument with a base pressure less than 1×10^{-9} Torr using MgK α (1253.6 eV) radiation. Photoelectrons were energy analyzed using 20 eV or 50 eV pass energies for region or survey scans, respectively, with a concentric hemispherical analyzer. The angle between the sample plane and the perpendicular to the entrance of the analyzer was 90°. To eliminate charging effects, the edges of the sample surfaces were electrically connected to the sample stub, which was at electrical ground, using vacuum-compatible silver paint. The contact angles of SAM-functionalized gold substrates and the PS and PAA films were measured by the sessile drop method using a Krüss model DSA-100 instrument for water, diiodomethane and ethylene glycol.

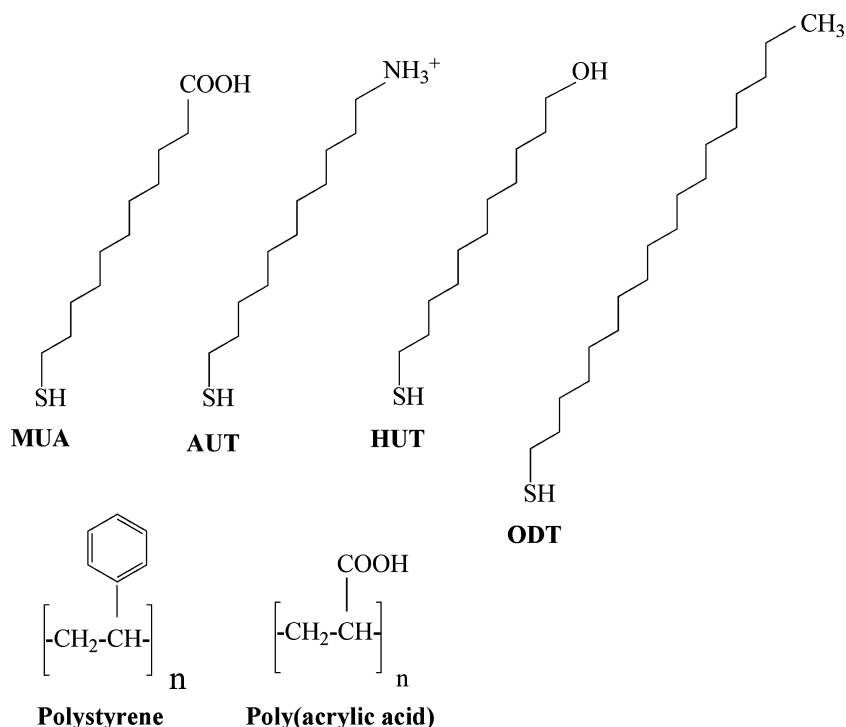


Fig. 1. Chemical structures of 11-mercaptoundecanoic acid (MUA), protonated 11-aminoundecanethiol (AUT), 11-hydroxyundecanethiol (HUT), octadecanethiol (ODT), polystyrene, and poly(acrylic acid).

2.2. Force measurements

All force measurements were performed with the Veeco Nanoscope IIIa AFM instrument. A homemade purging chamber was used to cover the AFM head, and the humidity was measured with a Vaisala M170 meter. Purging with N₂ gas was initiated 1–2 h before the force measurements. The relative humidity was below 0.5% during the experiments. The ramp size and scan rate for force measurements were 500 nm and 465 nm/sec, respectively. The AFM tip was cycled 50–60 times at the same sample location. Adhesive forces were calculated by processing the recorded force curves using SPIP software.

Force constants of the cantilevers were calculated using the Sader (10) treatment in which the force constant (k) is given by:

$$k = 0.1906 b^2 L Q_f \rho_f \Gamma_i(\omega_f) \omega_f^2 \quad (1)$$

where b , L , Q_f , ρ_f , ω_f and $\Gamma_i(\omega_f)$ are, respectively, the width and length of the cantilever (in μm), the quality factor of the cantilever oscillation, the density of the fluid (g/cm^3), the fundamental resonant frequency of the cantilever (kHz), and the imaginary component of the hydrodynamic function Γ . Field-effect scanning electron microscopy was used to measure the cantilever dimensions, and the resonant frequency and quality factor were measured by the in-built functions of the Veeco AFM software. The radius of the AFM tip was determined by scanning a silicon calibration grating (Mikromasch TGT01) comprised of tips having radii less than 10 nm. Because these tips were significantly smaller than the AFM tips used in the experiments, the radii of the AFM probes could be directly determined from the scanned images.

3. Results and discussion

3.1. Characterization of polymer surfaces and alkanethiol monolayers

The roughness of the prepared polymer films was measured by AFM imaging in tapping mode using a silicon nitride tip. The measured root mean square (rms) roughness was 0.17 and 0.23 nm for the PAA and PS films, respectively, confirming the formation of smooth surfaces. XPS was used to verify that the polymer film homogeneously covered the Si(111) substrates without leaving bare regions. Figure 2 shows “survey” scans of the PS and PAA films. Since XPS measures 50–100 Å deep, the absence of Si 2p signal at ca. 103–104 eV confirmed that the prepared films were uniformly thicker than the detection depth.

Because XPS cannot analyze nanometer-size samples, it is not possible to directly measure spectra of the monolayers adsorbed on the gold-coated tip. However, to confirm that the procedures used to prepare thiol layers on the tips yielded functionalized substrates, macro-scale samples were prepared with the same modification procedures used

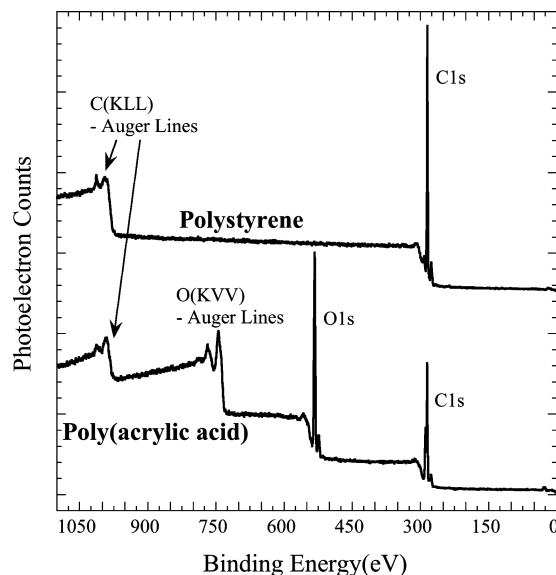


Fig. 2. MgK α XPS survey scans of the polystyrene and poly(acrylic acid) films spin-coated on silicon wafers. The absence of Si 2p signal confirms the formation of films thick enough to uniformly cover the silicon substrate.

for the gold-coated AFM tips. Specifically, gold-coated silicon wafers were UV ozone-treated and immersed in hot ethanol prior to SAM formation, as described earlier. XPS scans were performed of the C 1s, S 2p, O 1s, N 1s, Cl 2p and Au 4f regions, and atomic percentages were calculated by dividing the peak areas by the appropriate sensitivity factors. Table 1 displays the atomic percentages of “clean” gold and the thiol-modified gold substrates, and these are compared to the theoretical ratios expected based on chemical composition of the adsorbate molecules. The results confirm successful assembly of the molecules on the gold surfaces and, by extrapolation, on the gold-coated AFM tips.

The chemical nature of the AUT monolayer was also investigated using XPS. Figure 3 shows its S 2p region compared to that of ODT. The complicated spectrum in the case of AUT is due to multilayer formation that does not occur to a significant extent for the other thiols. As

Table 1. Surface concentrations (in atomic percentages) of the thiol-functionalized gold surfaces determined from XPS, the experimental atomic ratios, and the theoretically expected ratios.

	Au (%)	C (%)	S (%)	O (%)	N (%)	C:S:O:N (Exptl)*	C:S:O:N (Theoretical)
Gold	96.3	3.7	—	—	—	—	—
ODT	35.9	60.7	3.4	0	—	95:5:0:0	94.7:5.3:0:0
MUA	37.6	49.0	3.5	9.9	—	79:6:16:0	78.6:7.1:14.3:0
AUT	25.3	53.7	5.8	10.1	5.1	72:8:14:7	84.6:7.7:0:7.7
HUT	51.3	48.5	4.1	5.1	—	84:7:9:0	84.6:7.7:7.7:0

*The measured ratios have been rounded to reflect only the number of digits that are significant in consideration of the experimental error.

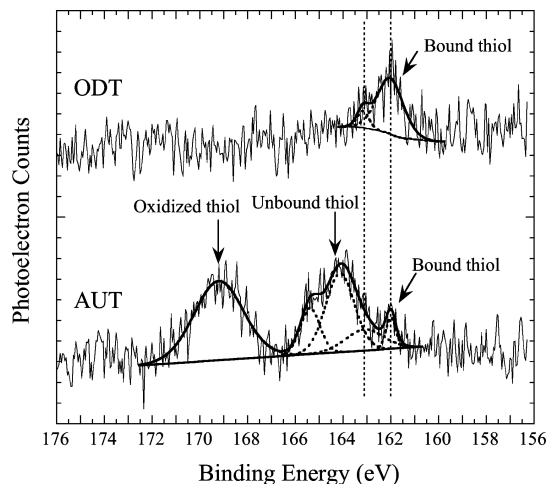


Fig. 3. MgK α XPS of the S 2p region of octadecanethiol (ODT) and 11-aminoundecanethiol (AUT) films adsorbed on gold substrates.

discussed in the experimental section, the AUT sample was rinsed several times with ethanol (as were the other samples) following immersion in the thiol solution. The XPS peak centered at 162.0 eV is due to thiolate sulfur atoms that result from S-Au bonding in the chemisorbed layer. The peaks at 164.1 and 165.3 eV are due to (intact) thiol groups in multilayer AUT, with the doublet arising from spin-orbit coupled peaks. The peak at 169.2 eV is attributed to oxidized sulfur. Note that the S 2p spectra of MUA and HUT (not shown) are similar to that of ODT. Amine-terminated thiols are susceptible to poor quality monolayer formation and, apparently, to oxidation of the thiol groups (11). The chemical composition data in Table 1 confirm the presence of oxygen in the films, and the relatively weak Au 4f signal compared to the other thiol films is consistent with multilayer formation leading to greater attenuation of the gold substrate signal.

Figure 4 shows the N 1s spectrum of the AUT sample. The major peak centered at 401.5 eV is attributed to ammonium ions, as observed for other amine-terminated self-assembled monolayers (12). The small component observed at ca. 400 eV is attributed to free (i.e., unprotonated) amine groups. Overall, therefore, the XPS results indicate that the AUT film is significantly different from the other thiol-functionalized surfaces and consists of several layers of AUT, with a large fraction containing oxidized thiol groups. A great majority of the AUT molecules are protonated due to R-NH₃⁺ formation. Note that no chlorine was detected by XPS in the AUT sample.

3.2. Contact angle measurements and surface free energy calculations

Contact angle measurements were performed to confirm the quality of the prepared organic films and to calculate their surface free energies. Table 2 displays water, ethylene

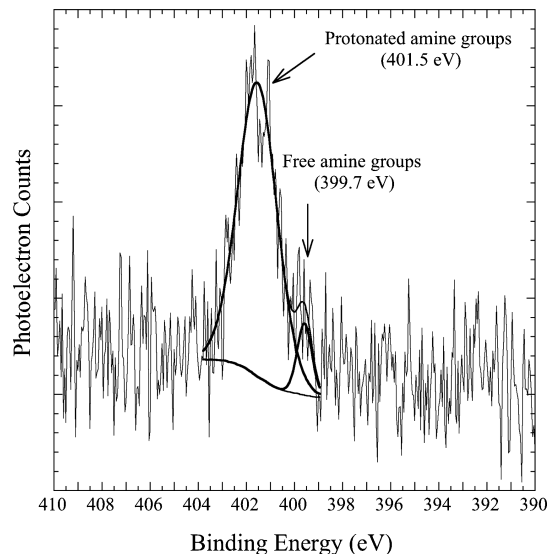


Fig. 4. MgK α XPS of the N 1s region of 11-aminoundecanethiol film adsorbed on gold. The peak at 401.5 eV indicates that the majority of the amine groups are protonated.

glycol, and diiodomethane contact angles of the various surfaces. Based on the water contact angle measurements, the hydrophilicity has the order: ODT < AUT < HUT < MUA. Using these data, the surface free energy (γ_s) of the thiol-functionalized gold and polymer surfaces may be determined from the following treatment (13,14). Contact angles may be related to the surface free energy at the solid-liquid interface by Young's equation:

$$\gamma_s = \gamma_{sL} + \gamma_L \cos \theta \quad (2)$$

where θ is the measured contact angle with the liquid of known surface free energy (γ_L), and γ_{sL} is the free energy of the solid-liquid interface. The total surface free energy (γ_s) of a solid surface is the sum of the dispersive (γ_s^d) and polar (γ_s^p) components.

$$\gamma_s = \gamma_s^d + \gamma_s^p \quad (3)$$

Using the geometric mean of the dispersive and polar components, the following equation is obtained:

$$\gamma_{sL} = \gamma_s + \gamma_L - 2(\gamma_s^d \gamma_L^d)^{1/2} - 2(\gamma_s^p \gamma_L^p)^{1/2} \quad (4)$$

Combination of equations (2) and (4) results in the so-called Owens-Wendt equation:

$$(1 + \cos \theta)\gamma_L = 2(\gamma_s^d \gamma_L^d)^{1/2} + 2(\gamma_s^p \gamma_L^p)^{1/2} \quad (5)$$

where θ is the measured contact angle with the liquid having known dispersive (γ_L^d) and polar (γ_L^p) components of the total surface energy (γ_L). Rearrangement of (5) leads to:

$$(1 + \cos \theta)\gamma_L / [2(\gamma_L^d)^{1/2}] = (\gamma_s^d)^{1/2} + (\gamma_s^p \gamma_L^p / \gamma_L^d)^{1/2} \quad (6)$$

The values for the dispersive and polar components of the free energies of the liquids used are known (15), and a

Table 2. Contact angles of functionalized gold substrates and polymer films and their surface free energies with estimated errors. The estimated error in contact angle measurements is $\pm 2^\circ$.

	Water (deg)	Ethylene glycol (deg)	Diiodomethane (deg)	γ_s^d (mJ/m ²)	γ_s^p (mJ/m ²)	$\gamma = \gamma_s^d + \gamma_s^p$ (mJ/m ²)
ODT	109	79	72	22.7 \pm 1.0	0.1 \pm 0.1	22.8 \pm 1.1
MUA	10	19	29	34.2 \pm 0.7	32.3 \pm 0.1	66.5 \pm 0.8
AUT	45	33	25	37.8 \pm 0.5	17.7 \pm 0.8	55.5 \pm 1.3
HUT	16	21	36	32.0 \pm 0.8	32.5 \pm 0.4	64.5 \pm 1.2
PS	91	60	36	39.9 \pm 0.8	0.6 \pm 0.2	40.5 \pm 1.0
PAA	5 ^a	—	29	44.6 ^b \pm 1.0	33.7 ^b \pm 0.3	78.3 ^b \pm 1.3

^aApproximate value.

^bBased on the assumption of a 5° PAA water contact angle.

linear plot of the left-hand side of Equation 6 vs. $(\gamma_L^p / \gamma_L^d)^{1/2}$ for the various solvents yields a slope of $(\gamma_s^p)^{1/2}$ and an intercept of $(\gamma_s^d)^{1/2}$.

In the case of PAA, difficulty arises measuring the contact angle of polar liquids because of dissolution of the film. In this case a water contact angle of 5° was assumed based on Ref. (16). Table 2 includes the total surface free energy of the various functionalized tips and polymer films using this analysis, along with the dispersive and polar components. For the hydrophobic ODT SAM and PS, the surface free energy is mainly composed of a dispersive component; for the other surfaces, the polar component accounts for a large fraction of the total free energy. For the hydrophilic monolayers, the following order of surface free energy is found: MUA > HUT > AUT. The measured contact angles and surface free energies are in general agreement with related literature values (17–20).

4. Force measurements on polymer surfaces

The interaction between functionalized AFM tips and polymer surfaces was measured via force-distance curves. The force measured during tip retraction is the adhesive force developed between the tip and substrate after contact. In air, capillary effects dominate, and the measured adhesive forces are not a true assessment of intermolecular forces. To eliminate capillary effects, all of the force measurements have been performed at a relative humidity of less than 0.5%. Each functionalized gold tip has been used to probe forces on both the PS and PAA surfaces in order to ensure that the tip radius is identical for comparative measurements between the two polymers. After performing measurements on the PS film, the tip was cleaned in ethanol and dried with nitrogen gas prior to making measurements on PAA. For each tip-sample combination, at least 50 “pull-off” force curves were recorded, and mean adhesive forces were calculated.

Figures 5 displays typical force curves for each functionalized tip on the two polymer films, and the average and standard deviation of the ca. 50 such measurements for each system are presented in Table 3. Because the measured

adhesive forces depend on the contact area, for comparison between different tip-sample combinations it is necessary to normalize the force by dividing it by the tip radius. These values are also included in Table 3. The largest normalized adhesive force observed for all combinations is for HUT/PAA, which gives a value of 1.24 N/m. This is reasonable since strong adhesive forces between OH and COOH groups are expected due to hydrogen bonding effects. The smallest normalized adhesive force (0.1 N/m) is observed for the ODT/PAA combination, consistent with the dissimilar hydrophilic natures of these two organic films.

To check the validity of our force measurements, we have calculated the theoretically expected adhesion force for the PS/ODT system. The normalized adhesive force (F/R) due to van der Waals attraction between a sphere (designated as “1”) and a flat plane (designated as “2”) may be calculated by DMT theory (21) as:

$$F/R = 2\pi W_{12} \quad (7)$$

where R is radius of the sphere (i.e., the AFM tip) and W_{12} is the work of adhesion. The work of adhesion may be approximated using the following equation:

$$W_{12} = A/[12\pi D_O] \quad (8)$$

where D_O is the cutoff separation, commonly assumed to be 0.165 nm (22), and A is the non-retarded Hamaker constant. The Hamaker constants, A_{PS} and A_{ODT} , for PS and ODT (approximated as a hydrocarbon) are taken as 6.5×10^{-20} and 7.1×10^{-20} J, respectively (22). The Hamaker constant of the PS/ODT system in air, which is A in Equation 8, is therefore $(A_{PS} \times A_{ODT})^{1/2}$ or 6.8×10^{-20} J. Using Equations 7 and 8, the theoretical work of adhesion between PS and ODT is 0.066 J/m² with an F/R value of 0.41 N/m. The experimental normalized adhesive force value of 0.49 N/m, which is 20% higher than the theoretical value. The reasonable agreement between the theoretical and experimental values for the ODT/PS system confirms the methods used in this paper.

The work of adhesion (W_{12}) for each system may be calculated from the experimentally measured normalized adhesion forces using Equation 7, and the values are in-

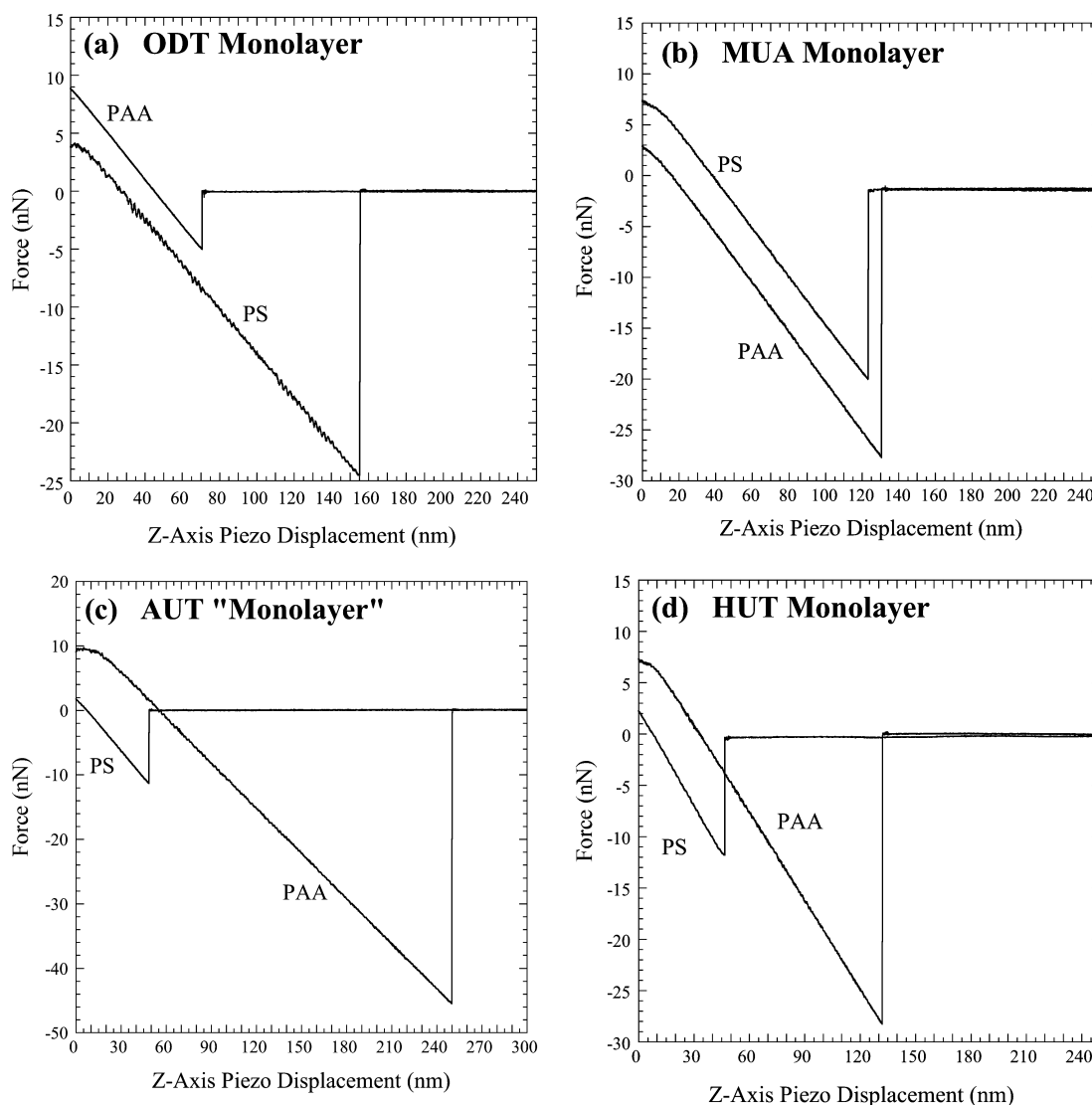


Fig. 5. Examples of pull-off curves from polystyrene and poly(acrylic acid) surfaces for AFM tips functionalized with a) octadecanethiol, b) 11-mercaptoundecanoic acid, c) 11-aminoundecanethiol, and d) 11-hydroxyundecanethiol.

cluded in Table 4. The interfacial free energies (γ_{12}) can be calculated from the works of adhesion using the Dupr e equation:

$$W_{12} = \gamma_1 + \gamma_2 - \gamma_{12} \quad (9)$$

Table 3. Measured adhesive and normalized adhesive forces for each tip-sample combination.

Tip radius (nm)	Polystyrene		Poly(acrylic acid)	
	F (nN)	F/R (N/m)	F (nN)	F/R (N/m)
ODT	25.3 ± 4.8	0.49 ± 0.09	5.2 ± 0.9	0.1 ± 0.02
MUA	19.0 ± 0.9	0.45 ± 0.02	26.5 ± 1.5	0.63 ± 0.04
AUT	9.4 ± 0.7	0.17 ± 0.01	49.7 ± 3.0	0.92 ± 0.06
HUT	9.3 ± 2.6	0.36 ± 0.10	32.3 ± 3.6	1.24 ± 0.14

where γ_1 and γ_2 are the surface free energies of the tip and substrate. The calculated values of the interfacial free energies are also included in the table. Note that negative γ_{12} values suggest that stronger interfacial bonds are

Table 4. Work of adhesion and interfacial free energy for each tip-sample combination using DMT theory.

	Polystyrene		Poly(acrylic acid)	
	W_{12} (mJ/m ²)	γ_{12} (mJ/m ²)*	W_{12} (mJ/m ²)	γ_{12} (mJ/m ²)*
ODT	78 ± 14	-15	16 ± 3	85
MUA	72 ± 3	34	100 ± 6	44
AUT	27 ± 2	69	146 ± 9	-12
HUT	57 ± 16	48	197 ± 22	-54

*The errors in the interfacial surface energy are estimated to be similar to the errors in the corresponding works of adhesion.

formed between the tip and substrate than within the tips or substrates themselves, as previously observed for other adhesive studies (23).

It is also interesting to examine the relative magnitudes of the works of adhesion. Assuming that the measured work of ca. $78 \pm 14 \text{ mJ/m}^2$ for the ODT/PS system is completely due to van der Waals interactions and that similar amounts exist for the other systems, it can (to a rough approximation) be estimated that the difference is due hydrogen bonding and ion-dipole interactions. For example, in the case of HUT/PAA, the work of adhesion due to hydrogen bonding is ca. 119 mJ/m^2 out of the total 197 mJ/m^2 . As discussed earlier, the AUT-functionalized surface contains NH_3^+ and most probably SO_3^- groups. These certainly play a role in increasing the work of adhesion to PAA through ion-dipole forces. It is also interesting that the measured work of adhesion for ODT/PAA is only 16 mJ/m^2 . This is almost 5 times lower than the value obtained for ODT/PS and clearly demonstrates that CH_3 -PS van der Waals forces are significantly stronger than CH_3 -PAA ones.

It should be noted that some error may arise in the above calculations due to the limitations of DMT theory. As discussed in Ref. (7), DMT theory is most applicable for systems with low adhesion probed using a small tip radius. Competing JKR theory (7,22) has advantages for highly adhesive systems probed with a large tip radius having low stiffness. While the experimentally measured work of adhesion for the ODT/PS system agrees with DMT theory, greater errors could arise in the measurements for highly adhesive systems such as HUT/PAA. Further work is needed to clarify these issues, especially in the case of polymer-coated surfaces.

5. Conclusions

The normalized adhesion forces have been measured for various thiol-modified gold tips contacting polystyrene and poly(acrylic acid) surfaces. In the case of polystyrene, the normalized adhesion forces follow the order: ODT > MUA > HUT > AUT. In the case of poly(acrylic acid), the normalized adhesion forces have the order: HUT > AUT > MUA > ODT. The work of adhesion has been calculated based on DMT theory, with the HUT/PAA system exhibiting a value of ca. 200 mJ/m^2 . In contrast, the ODT/PAA system exhibits a work of adhesion that is an order of magnitude lower.

Acknowledgments

This work was supported by the Center for High-Rate Nanomanufacturing at the University of Massachusetts Lowell as part of National Science Foundation Grant No. NSF-0425826.

References

1. Myers, D. *Surfaces, Interfaces, and Colloids: Principles and Applications*; VCH: New York, 1991.
2. Alfano, J.C., Carter, P.W., Nowak, M.J. and Whitten, J.E. (1999) Coagulant Mediation of Interfacial Forces Between Anionic Surfaces. *Nordic Pulp Pap. Res. J.*, 14: 30–36.
3. Simson, R. and Sackmann, E. Mimicking Physics of Cell Adhesion. In *Physical Chemistry of Biological Interfaces*; Baszkin, A., Norde, W., Eds.; Marcel Dekker, Inc.: New York, 401–430, 2000.
4. Chandekar, A., Sengupta, S.K., Barry, C.M.F., Mead, J.L. and Whitten, J.E. (2006) Template-Directed Adsorption of Block Copolymers on Alkanethiol-Patterned Gold Surfaces. *Langmuir*, 22: 8071–8077.
5. Chandekar, A., Sengupta, S.K. and Whitten, J.E. (2007) Template-Directed Patterning of Polymers and Biomaterials. *Micros. Res. Tech.*, 70: 506–512.
6. Chandekar, A. and Whitten, J.E. (2007) Nanoscale Patterning of a Conjugated Oligomer. *Appl. Phys. Lett.*, 91: 113103–113106.
7. Cappella, B. and Dietler, G. (1999) Force-Distance Curves by Atomic Force Microscopy. *Surf. Sci. Rep.*, 34: 1–104.
8. Noy, A., Frisbie, C.D., Rozsnyai, L.F., Wrighton, M.S. and Lieber, C.M. (1995) Chemical Force Microscopy: Exploiting Chemically-Modified Tips to Quantify Adhesion, Friction, and Functional Group Distributions in Molecular Assemblies. *J. Am. Chem. Soc.*, 117: 7943–7951.
9. Fujihira, M., Okabe, Y., Tani, Y., Furugori, M. and Akiba, U. (2000) A Novel Cleaning Method of Gold-Coated Atomic Force Microscope Tips for the Chemical Modification. *Ultramicroscopy*, 82: 181–191.
10. Sader, J.E., Chon, J.W.M. and Mulvaney, P. (1999) Calibration of Rectangular Atomic Force Microscope Cantilevers. *Rev. Sci. Instr.*, 70: 3967–3969.
11. Wang, H., Chen, S., Li, L. and Jiang, S. (2005) Improved Method for the Preparation of Carboxylic Acid and Amine Terminated Self-Assembled Monolayers of Alkanethiolates. *Langmuir*, 21: 2633–2636.
12. Hooper, A.E., Werho, D., Hopson, T. and Palmer, O. (2001) Evaluation of Amine- and Amide-Terminated Self-Assembled Monolayers as ‘Molecular Glues’ for Au and SiO_2 Substrates. *Surf. Interface Anal.*, 31: 809–814.
13. Owens, D.K. and Wendt, R.C. (1969) Estimation of the Surface Free Energy of Polymers. *J. Appl. Poly. Sci.*, 13: 1741–1747.
14. Fowkes, F.M. (1962) Determination of Interfacial Tensions, Contact Angles, and Dispersion Forces in Surfaces by Assuming Additivity of Intermolecular Interactions in Surfaces. *J. Phys. Chem.*, 66: 382.
15. Bouali, B., Ganachaud, F., Chapel, J.-P., Pichot, C. and Lanteri, P. (1998) Acid-Base Approach to Latex Particles Containing Specific Groups Based on Wettability Measurements. *J. Colloid Int. Sci.*, 208: 81–89.
16. Yoo, D., Shiratori, S.S. and Rubner, M.F. (1998) Controlling Bilayer Composition and Surface Wettability of Sequentially Adsorbed Multilayers of Weak Polyelectrolytes. *Macromolecules*, 31: 4309–4318.
17. Awada, H., Castelein, G. and Brogly, M. (2005) Quantitative Determination of Surface Energy Using Atomic Force Microscopy: The Case of Hydrophobic/Hydrophobic Contact and Hydrophilic/Hydrophilic Contact. *Surf. Int. Anal.*, 37: 755–764.
18. Noel, O., Brogly, M., Castelein, G. and Schultz, J. (2004) In Situ Determination of the Thermodynamic Surface Properties of Chemically Modified Surfaces on a Local Scale: An Attempt with an Atomic Force Microscope. *Langmuir*, 20: 2707–2712.
19. Ahn, H.-S., Cuong, P.D., Park, S., Kim, Y.-W. and Lim, J.-C. (2003) Effect of Molecular Structure of Self-Assembled Monolayers on their Tribological Behaviors in Nano- and Microscales. *Wear*, 255: 819–825.

20. Tsukruk, V.V. and Bliznyuk, V.N. (1998) Adhesive and Friction Forces between Chemically Modified Silicon and Silicon Nitride Surfaces. *Langmuir*, 14: 446–456.
21. Derjaguin, B.V., Muller, V.M. and Toporov, Y.P. (1975) Effect of Contact Deformations on the Adhesion of Particles. *J. Colloid Int. Sci.*, 53: 314–325.
22. Israelachvili, J. *Intermolecular & Surfaces Forces*; Academic Press: London, 1992.
23. Thomas, R.C., Houston, J.E., Crooks, R.M., Kim, Taisun and Michalske, T.A. (1995) Probing Adhesion Forces at the Molecular Scale. *J. Am. Chem. Soc.*, 117: 3830–3834.